Antiferromagnetic Fluctuations and Short-Range Order in a Kagomé Lattice

C. Broholm, G. Aeppli, G. P. Espinosa, and A. S. Cooper
AT&T Bell Laboratories, Murray Hill, New Jersey 07974
(Received 7 March 1990)

We report neutron-scattering measurements on $SrCr_{8-x}Ga_{4+x}O_{19}$, a layered compound containing Kagomé planes of $S=\frac{3}{2}$ Cr^{3+} ions. From magnetic-susceptibility data, the Curie-Weiss constant is large and negative, $\theta_{CW}\cong -500$ K. Even so, our measurements for a sample with $x=0.87$ reveal only short-range antiferromagnetic order with a correlation length $\xi=7\pm 2$ Å $\approx 2a$, where a is the inter-Cr spacing. Below 8 K, there is a spin-freezing transition to a state where the magnetic fluctuations have large amplitude and a spectrum (averaged over reciprocal space) characteristic of two-dimensional antiferromagnets with $\xi \gg a$.

PACS numbers: 75.40.Gb, 75.25.+z, 75.50.Lk

There are very few simple two-dimensional magnets which fail to order at $T=0$. For example, the $S=\frac{1}{2}$ nearest-neighbor-coupled Heisenberg antiferromagnet (AFM) orders not only on a square lattice[1] but also on a triangular lattice,[2] which is perhaps the best-known geometrically frustrated lattice. Among structurally ordered systems with vanishing further-neighbor interactions which remain candidate hosts for magnetic ground states with finite two-spin correlation lengths are antiferromagnets on Kagomé lattices.[3] Figure 1(a) shows a Kagomé lattice, which is a triangular lattice, with lattice parameter a, where vacancies have been introduced at all sites of a triangular superlattice, with lattice parameter $2a$. For AFM-coupled Ising spins on a Kagomé lattice, there is no phase transition and AFM correlations decay exponentially even at $T=0$ with a finite correlation length $\xi=3.3a$.[4] For classical as well as quantum Heisenberg and x-y spins, less is known theoretically, but for these cases also, the Kagomé lattice is expected to host highly degenerate and possibly short-range-ordered ground states.[5] The discovery that the layered oxide $SrCr_{8-x}Ga_{4+x}O_{19}$ [SCGO(x)] contains AFM-interacting Cr^{3+} ($S=\frac{3}{2}$) ions on a Kagomé lattice has made an experimental approach to the Heisenberg Kagomé AFM possible. Obradors *et al.*[6] showed that despite a Curie-Weiss temperature of -492 K, long-range magnetic order is absent above 4.2 K.[7] Ramirez, Espinosa, and Cooper[8] discovered spin-glass transitions at temperatures T_g^{bulk} between 3.5 and 7 K, depending on the value for x. In the present paper, we describe neutron-scattering data which establish that the correlations in this compound are very short ranged ($\xi\cong 7$ Å) and associated with local order of the type also found in the triangular AFM. Furthermore, our data are consistent with spin freezing for $T<T_g^{bulk}=5$ K. What is most fascinating, however, is that well within the spin-glass state, fluctuations account for a net magnetic moment in excess of twice the frozen moment. Also, in spite of the small ξ, the local magnetic fluctuations resemble those in an ordered two-dimensional Heisenberg AFM.

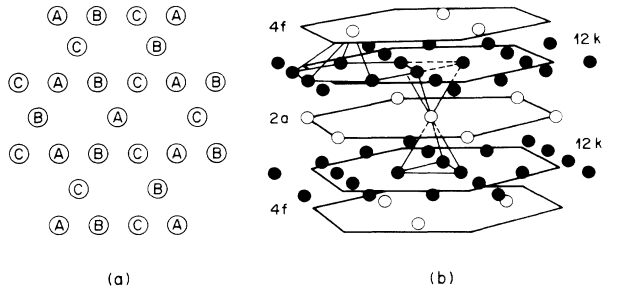

FIG. 1. (a) Kagomé lattice with three-sublattice order indicated by letters A, B, and C. (b) Locations of Cr atoms (solid and open circles) in SCGO(x). $12k$ layers containing solid circles are Kagomé planes.

Figure 1(b) shows the Cr^{3+} sites of SCGO(x) (Ref. 6) which form a stack of dense Kagomé lattices (labeled $12k$) separated by more dilute triangular lattices ($2a$ and $4f$). Surrounded by weakly distorted oxygen octahedra the magnetic moment of Cr^{3+} is a good realization of an $S=\frac{3}{2}$ Heisenberg spin.[9] Our powder sample was made by cooling $SrCO_3$, Cr_2O_3, and Ga_2O_3 in a SrO-B_2O_3 solvent. The neutron powder-diffraction pattern at $T=1.5$ K was consistent with the hexagonal crystal structure previously reported[6] with lattice parameters $a'=2a=5.80$ Å and $c=22.7$ Å except for one Bragg peak, ascribed to 5 wt% of nonreacted Cr_2O_3. Since the Bragg intensities were independent of sample rotation, the distribution of grain orientations was isotropic. Susceptibility measurements showed that $x=0.87$ for our sample,[8] corresponding to Cr concentrations (extrapolated from the $x=0$ sample[6]) of 80%, 90%, and 80% for the $12k$, $2a$, and $4f$ sites, respectively. Since the Cr concentration in all layers is well above the 2D site-percolation threshold (65.27% for the Kagomé lattice, 50% for the triangular lattice[3]) dilution does not limit the correlation length, but the associated randomness may be responsible for the system undergoing a spin-glass transition instead of remaining paramagnetic to lower temperatures.

We performed double- and triple-axis neutron-scattering measurements using the TAS-1 instrument at Risø National Laboratory, Denmark. For energy trans-

fers $\hbar\omega$ in the ranges 0.18–0.7, 0.4–1.8, and 2–8 meV, the fixed incident energies E_i were 3.6, 5, and 13.9 meV, yielding energy resolutions ΔE of 0.1, 0.2, and 1.2 meV (FWHM), respectively. Data taken with different spectrometer configurations were normalized using the (002) powder reflection of SCGO(x) as a standard.

Previous workers[6] found no magnetic Bragg scattering for $T > 4.2$ K. Our two-axis measurements show that this remains the case to 1.5 K. Nevertheless, Fig. 2(a) reveals that in addition to nuclear Bragg peaks (off scale) and small-angle scattering, there is a broad maximum centered at $Q_0 = 1.4$ Å$^{-1} \cong (1/\sqrt{3})a^*$ ($a^* = 4\pi/\sqrt{3}a$), the location of the lowest-order superlattice spots $\mathbf{Q}_0 = (\frac{1}{3}, \frac{1}{3})$ associated with three-sublattice ordering[10] in the triangular parent of the Kagomé lattices in SCGO(x). In Fig. 1(a), the letters A, B, and C represent the corresponding sublattices projected onto the Kagomé lattice. For the x-y and Heisenberg models, A, B, and C refer to spins 120° apart in a single plane. Since the scattered neutron energies were not analyzed, the maximum in the scattering of Fig. 2(a) arises from AFM correlations which persist on a time scale given by $E_i = 5$ meV $= 1.2$ THz. The difference plot in Fig. 2(b) shows that this scattering, and hence the correlation length and amplitude of the associated magnetic fluctuations, is temperature independent between 10 and 1.5 K.

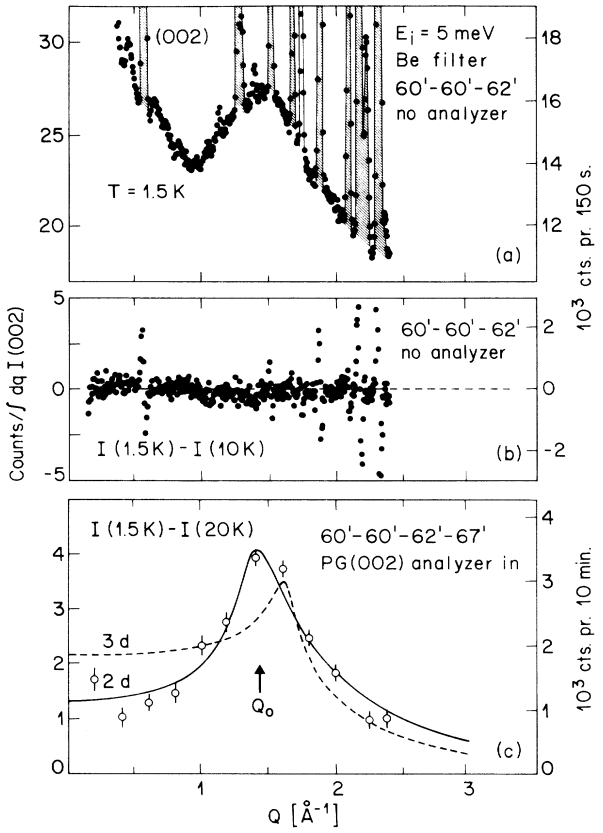

FIG. 2. (a) Two-axis (no final-energy analysis) scattering intensity vs elastic momentum transfer Q. Nuclear Bragg peaks of SCGO(x) (mostly off scale) are crosshatched. The nonhatched Bragg peak at 1.73 Å^{-1} is (110) of Cr_2O_3. (b) Difference between two-axis data taken at 1.5 and 10 K. Close to strong nuclear Bragg peaks, spectrometer-setting errors give rise to sharp deviations from zero. (c) Difference between elastic signals measured by three-axis spectroscopy.

We can study correlations which persist on a longer time scale by installing an analyzer, and measuring nominally elastic scattering. At 1.5 K, there is also a maximum at Q_0 in the elastic scattering, which disappears on raising T. Figure 2(c) shows the Q-dependent difference between the 1.5- and 20-K data; note that the normalized amplitude is roughly one-third that found in the two-axis experiment. Thus we have established that spin components which are frozen on the time scale corresponding to our experimental resolution (0.2 meV = 50 GHz) appear between 20 and 1.5 K, but account for only a small part of the AFM correlations in SCGO(x). Figure 3 shows the temperature dependence of this elastic scattering at $Q = Q_0$. With decreasing T, there is an increase in the signal due to critical slowing down followed by spin freezing.[11] While the intensity increases most dramatically at 8 K, hysteresis in the dc susceptibility of our sample is found below $T_g^{\text{bulk}} = 5$ K.[8] That the temperatures at which anomalies occur depend on the time scale of the measurement is a well-known property of spin glasses.

The Q-dependent elastic scattering in the frozen state is well described by the powder average of a 2D Lorentzian, $S(\mathbf{Q}) \sim 1/(\xi^2|\mathbf{Q}_\perp - \mathbf{Q}_0|^2 + 1)$, where only the basal-plane components $\mathbf{Q}_\perp$ of $\mathbf{Q}$ enter. The solid line in Fig. 2(c) is the best fit with this form multiplied by the magnetic form factor of Cr^{3+} and assuming the isotropic polarization factor relevant for Heisenberg spins. Whereas good fits can also be obtained for 2D correlations with planar or axial anisotropy, our data are inconsistent with isotropic 3D correlations (dashed line). The 2D correlation length deduced from the fit is $\xi = 7$

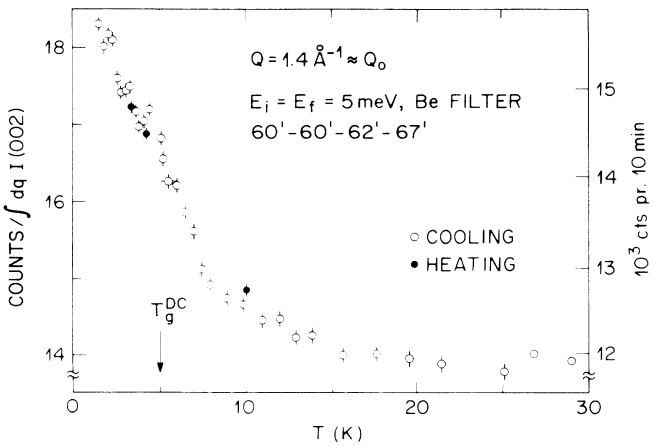

FIG. 3. Temperature dependence of elastic intensity at $Q = 1.4$ Å$^{-1} \approx Q_0$.

± 2 Å, only twice the inter-Cr spacing in the Kagomé planes. Allowing for a finite out-of-plane correlation length $\xi_{\|}$ yields somewhat better fits with the in-plane correlation length $\xi = 9 \pm 2$ Å and $\xi_{\|} = 1.5 \pm 0.6$ Å. The effective two dimensionality of SCGO(x) is presumably due both to the 3-times-lower Cr^{3+} concentration in the triangular-lattice planes which separate Kagomé planes and to the frustration of interactions between spins occupying different planes.

Figure 4 shows $\chi''(Q,\omega)$, the imaginary part of the dynamical susceptibility obtained via the fluctuation-dissipation theorem from constant-$\hbar\omega$ and -Q scans which measure $S(Q,\omega)$ for our powder sample. For fixed Q, $\chi''(Q,\omega)$ decreases only by a factor of 2 between the lowest (0.2 meV) and highest $\hbar\omega$ (8 meV) accessed. Furthermore, the Q dependence of $\chi''(Q,\omega)$ is roughly independent of $\hbar\omega \leq 8$ meV and similar to that of the elastic scattering. Both results confirm expectations that the energy scale for the interactions giving rise to the AFM correlations is much larger than 8 meV. Constant-$\hbar\omega$ scans could also be fitted by powder-averaged 2D Lorentzians (solid lines). The corresponding ξ decreases with increasing $\hbar\omega$ in a manner describable by $\xi^{-2} = \xi_0^{-2} + (\omega/c)^2$, where $\xi_0 = 6 \pm 1$ Å, in agreement with the correlation length for elastic scattering, and $\hbar c \geq 40$ meV Å. Thus, as for low-dimensional systems and other materials with strong fluctuations, magnetic correlations are apparent at frequencies much larger than the ordering (freezing) temperature. In this context, an important number is the ratio of the mean squares of the fluctuating $\langle|\Delta\mu|^2\rangle$ and frozen $|\langle\mu\rangle|^2$ moments. Applying the total-moment sum rule to our normalized inelastic (Fig. 4) and elastic [Fig. 2(c)] data we obtain the lower bound $\langle|\Delta\mu|^2\rangle/|\langle\mu\rangle|^2 > 4$. For comparison, $\langle|\Delta\mu|^2\rangle/|\langle\mu\rangle|^2 \approx 0.45$ for the $S = \frac{1}{2}$ Heisenberg AFM on a square lattice.[1] Note that we determine the moment frozen on the time scale given by our energy resolution (0.2 meV = 50 GHz), so our data are also consistent with the absence of truly elastic scattering, i.e., $\langle\mu\rangle = 0$, in which case the ground state could be regarded as a spin liquid.

While the high-frequency fluctuations in SCGO(x) are unusual for their amplitude, the low-frequency portion of $\chi''(Q,\omega)$ is peculiar for its ω dependence. Both because of the automatic averaging associated with our powder sample and because the Q dependence of $\chi''(Q,\omega)$ changes little, if at all, with $\hbar\omega \leq 5$ meV, $\chi''(Q_0,\omega)$ is a good measure of the local response function,

$$\chi_0''(\omega) = \int \chi''(\mathbf{q},\omega)\,d\mathbf{q} = 4\pi \int \chi''(Q,\omega) Q^2\,dQ\,.$$

For simple paramagnets where a single (exponential) relaxation process dominates at long times, $\chi''(\omega) \sim \omega$ at small ω. On the other hand, for reasons described in more detail below, ordered two-dimensional antiferromagnets (at $T = 0$) yield local response functions which are constant at small ω. Figure 5 shows that $\chi_0''(\omega)$ for SCGO(x) evolves between these two limits upon lowering T through T_g. Indeed, a power law ω^α (solid lines) gives a good account of $\chi''(Q_0,\omega)$ for $0.2 < \hbar\omega \leq 2$ meV; thus, the low-temperature state is associated with $\alpha \to 0$, i.e., the appearance of a frequency independent $\chi_0''(\omega)$.

The response function $\chi_0''(\omega)$ is not simply the spectral density $\rho(\omega)$ of excited states, but involves the matrix elements of the spin operator (S_j) at each site (j) between the ground and excited states. More precisely, at $T = 0$,

$$\chi_0''(\omega) = \sum_j \sum_f |\langle f|S_j|0\rangle|^2 \delta(E_f - \hbar\omega)\,,$$

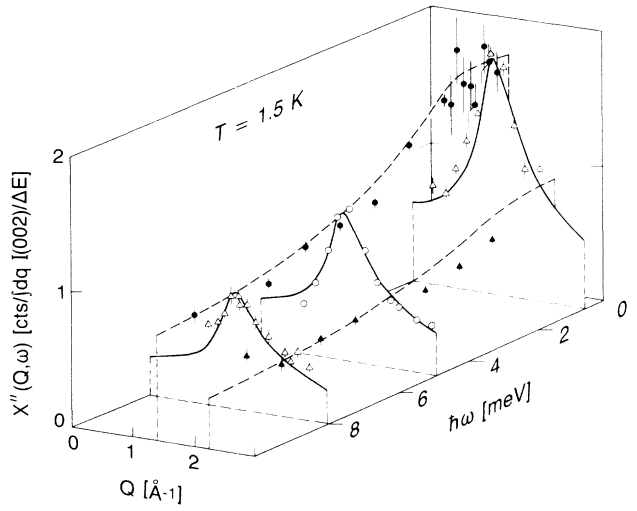

FIG. 4. Overview of Q- and ω-dependent magnetic response at $T = 1.5$ K $\ll T_g$. Open symbols are with constant $\hbar\omega$; solid symbols, with constant Q. Solid lines are from fits described in the text.

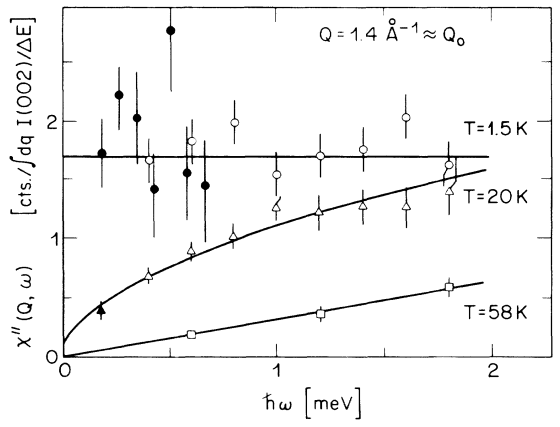

FIG. 5. $\chi''(Q_0,\omega)$ for $\hbar\omega \leq 2$ meV at three temperatures. Solid lines represent best fits with power laws ω^α. The solid points were measured with $E_i = 3.6$ meV. For open symbols, $E_i = 5$ meV.

whereas $\rho(\omega)=\sum_f \delta(E_f-\hbar\omega)$; the mean-square matrix element at a particular frequency is simply defined as $\langle M^2(\omega)\rangle=\chi_0''(\omega)/\rho(\omega)$. For ordinary spin glasses, where from specific-heat measurements $\rho(\omega)\sim$const at small ω (Ref. 12) and $\alpha\approx 0$,[13] $\langle M^2(\omega)\rangle\rightarrow$ const as $\omega\rightarrow 0$. On the other hand, for ordered Heisenberg AFM's, $\langle M^2(\omega)\rangle\sim 1/\omega$ because of the diverging overlap between the Néel state with a single flipped spin and spin waves with energy $\hbar\omega\rightarrow 0$,[14] with the result that in 2D $\alpha=0$ even though $\rho(\omega)\sim\omega$. It is surprising that SCGO(x), with its small ξ and spin-glass-like properties, also has $\rho(\omega)\sim\omega$ [because $C(T)\sim T^2$ at low T (Ref. 8)] and $\alpha\approx 0$, which makes SCGO(x) at the presently accessed frequencies resemble more the long-range-ordered 2D AFM than conventional spin glasses. This similarity, while *not* implying the presence of propagating modes in SCGO(x), does lead us to speculate that the magnetic fluctuations emanate from a ground state with long-range order in a continuous degree of freedom not directly visible by neutron scattering. Various kinds of order (e.g., "spin nematic" and "chiral") which satisfy this requirement have arisen recently in theories of frustrated 2D magnets.[15] Adaptation of the three-sublattice structure of the triangular Heisenberg and x-y AFM to the Kagomé AFM indicates that the correlation length defined as the distance between neighboring spins which do not form 120° angles with each other can diverge while maintaining a short two-spin correlation length.[16] Whether this is indeed the case for spins in the Kagomé planes of SCGO(x) will require further measurements, especially on single crystals.

We are grateful to E. Bucher for bringing SCGO(x) to our attention, P. Chandra, P. Coleman, D. Huse, A. P. Ramirez, and C. M. Varma for helpful discussions, and the staff at Risø National Laboratory for its hospitality during the measurements.

[1]S. D. Reger and A. P. Young, Phys. Rev. B **37**, 5978 (1988); R. R. P. Singh, Phys. Rev. B **39**, 9760 (1989).

[2]D. A. Huse and V. Elser, Phys. Rev. Lett. **60**, 2531 (1988).

[3]I. Syozi, Prog. Theor. Phys. **6**, 306 (1951); I. Syozi, in *Phase Transitions and Critical Phenomena*, edited by C. Domb and M. S. Green (Academic, New York, 1972), Vol. 1, p. 269; R. Liebmann, *Statistical Mechanics of Periodic Frustrated Ising Systems* (Springer-Verlag, Berlin, 1986), and references therein.

[4]A. Süto, Helv. Phys. Acta **54**, 191 (1981); **54**, 201 (1981).

[5]V. Elser, Phys. Rev. Lett. **62**, 2405 (1989); I. Ritchey and P. Coleman, Bull. Am. Phys. Soc. **35**, 800 (1990).

[6]X. Obradors *et al.*, Solid State Commun. **5**, 189 (1988). There is a misprint in Table 1: Sr is in 2D positions.

[7]Absence of long-range magnetic order has also been reported in other concentrated but potentially disordered frustrated AFM: M. Steiner *et al.*, J. Phys. Soc. Jpn. Suppl. **52**, 173 (1983); C. Pappa *et al.*, J. Phys. (Paris) **46**, 637 (1985); J. E. Greedan *et al.*, J. Appl. Phys. **67**, 5967 (1990).

[8]A. P. Ramirez, G. P. Espinosa, and A. S. Cooper, Phys. Rev. Lett. **64**, 2070 (1990).

[9]A. Abragam and B. Bleaney, *Electron Paramagnetic Resonance of Transition Ions* (Clarendon, Oxford, 1970).

[10]H. Kadowaki *et al.*, J. Phys. Soc. Jpn. **56**, 4027 (1987).

[11]A. P. Murani and A. Heidemann, Phys. Rev. Lett. **41**, 1402 (1978), give a detailed description of how neutron scattering establishes spin freezing.

[12]D. Meschede *et al.*, Phys. Rev. Lett. **44**, 102 (1980); L. E. Wenger and P. H. Keesom, Phys. Rev. B **13**, 4053 (1976).

[13]C. C. Paulsen *et al.*, Phys. Rev. Lett. **59**, 128 (1987).

[14]See G. Aeppli *et al.*, Phys. Rev. Lett. **62**, 2052 (1989), for an experimental confirmation in La_2CuO_4.

[15]P. Chandra and P. Coleman, Rutgers University Report No. 90-18, 1990 (unpublished); J. Villain, J. Phys. C **10**, 1717 (1977); W. G. Wen *et al.*, Phys. Rev. B **39**, 11413 (1989).

[16]G. Aeppli, C. Broholm, and A. P. Ramirez, in Proceedings of the Yamada Conference on Magnetic Phase Transitions, Osaka, 1990 (to be published).